1D Manganese(II) Derivatives of an Imidazole-Substituted Nitronyl Nitroxide. An Approach toward Molecular Magnetic Materials of High Dimensionality

Karine Fegy, Dominique Luneau, Elie Belorizky, Miguel Novac, Jean-Louis Tholence, Carley Paulsen, Thorsten Ohm, and Paul Rey*

Département de Recherche Fondamentale sur la Matière Condensée, Service de Chimie Inorganique et Biologique, Laboratoire de Chimie de Coordination (URA CNRS 1194), CEA-Grenoble, 17 rue des Martyrs, 38054 Grenoble Cédex 09, France, Laboratoire de Spectrométrie Physique (CNRS-UMR 5588), Université Joseph Fourier Grenoble 1, BP 87, 38402 Saint Martin d'Hères Cedex, France, and Centre de Recherche sur les Très Basses Températures, CRTBT-CNRS, BP166, 38042 Grenoble Cedex 09, France

Received December 29, 1997

Extended linear complexes of manganese(II) with a bis-chelating nitronyl nitroxide ligand, 2-(2-imidazolato)-4,4,5,5-tetramethyl-4,5-dihydro-1*H*-imidazolyl-3-oxide-1-oxy (NITIm), have been prepared where metallic and organic spin carriers alternate. Depending on the deprotonating agent, the solvent, and the counteranion, the species $[Mn(NITIm)(H_2O)_2]CH_3COO$, **1**, $[Mn(NITIm)(DMSO)_2]BPh_4$, **2**, $[Mn(NITIm)(H_2O)(ImH)]NO_3$, **3**, and $[Mn(NITIm)(NITImH)]ClO_4$, **4**, have been obtained, which differ by the additional ligands completing the metal coordination sphere. Complexes **1**−**3** are cis isomers and **4** is found as the *mer* modification; in all compounds, one observes a regular alternation of Λ and Δ metal environments. Their magnetic properties are similar, with Mn(II)−nitroxide interactions $J \approx -45$ cm^{-1} ($H = -2J\mathbf{S}_i\cdot\mathbf{S}_j$), and they display weak ferromagnetic properties below 5 K. Canting of the manganese ions is responsible for these properties. Relevant crystallographic parameters are as follows: **1**, space group *Fdd*2, $a = 16.713(1)$, $b = 40.111(3)$, $c = 9.735(1)$, $Z = 16$; **2**, space group $Pca2_1$, $a = 30.328(3)$, $b = 13.422(1)$, $c = 9.589(1)$, $Z = 4$; **3**, space group $P2_1/c$, $a = 9.787(2)$, $b = 22.973(5)$, $c = 9.671(2)$, $\beta = 117.32(3)°$, $Z = 4$; **4**, space group $P2_1/c$, $a = 9.761(2)$, $b = 28.668(5)$, $c = 9.941(2)$, $\beta = 96.07(3)°$, $Z = 4$.

Among several parameters, macroscopic properties in molecular magnetic materials depend on the dimensionality of the molecular frameworks and on the magnitude of the exchange coupling between the spin carriers.[1] Only a few species have been described which order ferro- or ferrimagnetically at room temperature, namely hexacyanometalates[2,3] and an adduct of vanadium and tetracyanoethylene.[4] In these compounds, a three-dimensional structure and a fairly strong exchange interaction are probably the cause of high-temperature magnetic ordering.

Most strategies aimed at designing molecular magnetic materials involve antiferromagnetically coupled alternating metal ions carrying spins of different moduli which do not compensate. These ferrimagnetic structures are assembled with polydentate bridging ligands such as oxalato, oxamato, oxamido, oximato, and dithiooxalato groups.[5] The use of these ligands has been fruitful, and several structures of high dimensionality have been reported, including a few three-dimensional examples where control over the chirality of the metal coordination sphere was achieved.[6−8] However, reported ordering temperatures are low because these materials include either diamagnetic bridging ligands, which do not efficiently mediate magnetic interactions, or diamagnetic metal ions.

Replacing diamagnetic ligands by paramagnetic nitronyl nitroxide free radicals seems to be an attractive strategy since large metal−nitroxide exchange interactions are warranted.[9] Indeed, coordination occurs through the spin density rich oxyl oxygen atom and exchange interactions ranging from strongly ferro- to strongly antiferromagnetic have been characterized. However, structures of high dimensionality are not readily obtained because crowded metal centers carrying electron-withdrawing groups are needed for coordination.[10] To overcome this difficulty, we investigated the coordination properties of chelating nitroxide ligands and found that the chelate effect was an efficient way to obtain strongly exchange coupled species using poorly acidic metal centers.[11,12]

Along this line, we report on the coordination properties of 2-(2-imidazolyl)-4,4,5,5-tetramethyl-4,5-dihydro-1*H*-imidazolyl-

* To whom correspondence should be addressed at CEA-Grenoble.

(1) Kahn, O. *Molecular Magnetism*; VCH: Cambridge, U.K., 1993.
(2) Mallah, T.; Thiebault, S.; Verdaguer, M.; Veillet, P. *Science* **1993**, *262*, 1554.
(3) Ferlay, S.; Mallah, T.; Ouahès, R.; Veillet, P.; Verdaguer, M. *Nature* **1995**, *378*, 701.
(4) Manriquez, J. M.; Yee, G. T.; McLean, R. S.; Epstein, A. J.; Miller, J. S. *Science* **1991**, *252*, 1415.
(5) Kahn, O. In *Molecular Magnetism: From Molecular Assemblies to the Devices*; Coronado, E., Delhaès, P., Gatteschi, D., Miller, J. S., Eds.; NATO ASI Series, No. 321; Kluwer Academic Publishers: Dordrecht, The Netherlands, 1996; p 243 and references therein.
(6) Decurtins, S.; Schmalle, H. W.; Schneuwly, P.; Oswald, H. R. *Inorg. Chem.* **1993**, *32*, 1888.
(7) Atovmyan, L. O.; Shilov, G. V.; Lyubovskaya, R. N.; Zhilyaeva, E. I.; Ovanesyan, N. S.; Pirumova, S. I.; Gusakovskaya, I. G.; Morozov, Y. G. *JETP Lett.* **1993**, *58*, 766.
(8) Decurtins, S.; Schmalle, H. W.; Oswald, H. R.; Linden, A.; Ensling, J.; Gütlich, P.; Hauser, A. *Inorg. Chim. Acta* **1994**, *216*, 65.
(9) Caneschi, A.; Gatteschi, D.; Rey, P. *Prog. Inorg. Chem.* **1991**, *39*, 331.
(10) Lim, Y. Y.; Drago, R. S. *J. Am. Chem. Soc.* **1971**, *93*, 891.
(11) Luneau, D.; Risoan, G.; Rey, P.; Grand, A.; Caneschi, A.; Gatteschi, D.; Laugier, J. *Inorg. Chem.* **1993**, *32*, 5616.
(12) Fegy, K.; Sanz, N.; Luneau, D.; Belorizky, E.; Rey, P. *Inorg. Chem.* **1998**, *37*, 4518.

S0020-1669(97)01619-4 CCC: $15.00
Published on Web 08/19/1998

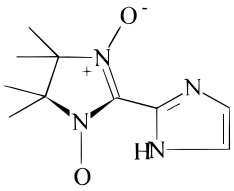

Figure 1. Chemical structure of the nitroxide ligand.

3-oxide-1-oxy (NITImH, Figure 1) in which deprotonation of the imidazole fragment provides possibilities for the coordination of both nitroxyl groups enforced by the chelate effect. In addition, since this bridging species is negatively charged, steric release of the metal center is also expected.

We report several 1D manganese(II) derivatives in which metal ions and bis-chelating free radical ligands alternate regularly. Moreover, in one of them, the metal coordination sphere is completed by another neutral radical ligand. This compound is the first example of a one-dimensional oligomeric metal−nitroxide complex where the metal coordination sphere is fully occupied by free radical ligands. Its local structural features and its magnetic properties are compared to those of the discrete tris(nitroxide)manganese(II) complex of the same ligand previously described[12] and to those of several closely related linear complexes which all have in common a bis-chelating bridging free radical ligand. At low temperature, one observes weakly antiferromagnetic interchain interactions which, in addition to weak local metal anisotropy, is responsible for the onset of weak hysteresis loops at low field and low temperature. These examples illustrate how functionalization of the nitronyl nitroxides is a promising strategy for building metal−nitroxide networks of high dimensionality.

Experimental Section

Syntheses. 2-(2-Imidazolyl)-4,4,5,5-tetramethyl-4,5-dihydro-1*H*-imidazolyl-3-oxide-1-oxy, NITImH, was prepared as described elsewhere.[13]

***catena*-Poly[diaquamanganese(II)-μ-[2-(2-imidazolato)-4,4,5,5-tetramethyl-4,5-dihydro-1*H*-imidazolyl-3-oxide-1-oxy-$\kappa O,\kappa N$:$\kappa O',\kappa N'$]-acetate], [[Mn(NITIm)$(H_2O)_2$](OAc)]$_n$, 1.** To a solution of 100 mg of NITImH (4.48×10^{-4} mol) and 21 mg of $Mn(NO_3)_2 \cdot 6H_2O$ (0.74×10^{-4} mol) in 5 mL of methanol was added a solution of 55 mg of $Mn(OAc)_2 \cdot 4H_2O$ (2.24×10^{-4} mol) in 5 mL of methanol. After the mixture was allowed to stand for 5 days in the dark at room temperature, the crystals that deposited were filtered off and dried under vacuum (75 mg, 45%). Anal. Calcd for [Mn(NITIm)$(H_2O)_2$]OAc, $C_{12}H_{21}N_4O_6$-Mn: C, 38.71; H, 5.68; N, 15.05. Mn, 14.75. Found: C, 38.47; H, 5.86; N, 14.90; Mn,14.52.

***catena*-Poly[bis(dimethyl sulfoxide)manganese(II)-μ-[2-(2-imidazolato)-4,4,5,5-tetramethyl-4,5-dihydro-1*H*-imidazolyl-3-oxide-1-oxy-$\kappa O,\kappa N$:$\kappa O',\kappa N'$]tetraphenylborate], [[Mn(NITIm)$(DMSO)_2$]-BPh_4]$_n$, 2.** In 5 mL of dimethyl sulfoxide were mixed 100 mg (4.48×10^{-4} mol) of NITImH, 73 mg (0.3×10^{-4} mol) of $Mn(OAc)_2 \cdot 4H_2O$, and 51 mg of sodium tetraphenylborate. Then 5 mL of methanol was added, and the mixture was left to stand in the dark at room temperature. The crystals that deposited were filtered off and dried (185 mg, 55%). Anal. Calcd for [Mn(NITIm)$(DMSO)_2$]BPh_4, $C_{38}H_{46}N_4O_4BS_2Mn$: C, 60.64; H,6.16; N, 7.44; B, 1.44; S, 8.52; Mn, 7.30. Found: C, 60.69; H, 6.09; N, 7.42; O, 8.51; B, 1.37; S, 8.56; Mn, 7.36.

***catena*-Poly[(imidazole)aquamanganese(II)-μ-[2-(2-imidazolato)-4,4,5,5-tetramethyl-4,5-dihydro-1*H*-imidazolyl-3-oxide-1-oxy-$\kappa O,\kappa N$:$\kappa O',\kappa N'$]nitrate hydrate], [[Mn(NITIm)(ImH)(H_2O)]$NO_3 \cdot H_2O$]$_n$, 3.** NITImH (100 mg, 4.48×10^{-4} mol) and $Mn(NO_3)_2 \cdot 6H_2O$ (86 mg, 3×10^{-4} mol) were dissolved in 5 mL of methanol. Then 31 mg of imidazole (4.48×10^{-4} mol) was added, and the solution was left to evaporate at room temperature in the dark. After 5 days, the crystals that formed (64 mg, 32%) were filtered off and dried under vacuum. Anal. Calcd for [Mn(NITIm)(ImH)]$NO_3 \cdot 2H_2O$, $C_{13}H_{22}N_7O_7Mn$: C, 35.22; H, 5.00; N, 22.12; Mn, 12.30. Found: C, 35.19; H, 5.15; N, 22.26; Mn, 11.69.

***catena*-Poly[[2-(2-imidazolyl-κN^3)-4,4,5,5-tetramethyl-4,5-dihydro-1*H*-imidazolyl-3-oxide-1-oxy-κO]manganese(II)-μ-[2-(2-imidazolato)-4,4,5,5-tetramethyl-4,5-dihydro-1*H*-imidazolyl-3-oxide-1-oxy-$\kappa O,\kappa N$:$\kappa O',\kappa N'$] perchlorate], [[Mn(NITIm)(NITImH)]ClO_4]$_n$, 4.** To a solution of 223 mg (10^{-3} mole) of NITImH in 80 mL of ethanol were added successively 181 mg (5×10^{-4} mol) of $Mn(ClO_4)_2 \cdot 6H_2O$ in 10 mL of ethanol and 34 mg (5×10^{-4} mol) of imidazole in 10 mL of ethanol. The dark blue solution was allowed to evaporate in the dark at room temperature. After 4 days, the crystals that deposited were collected by filtration and dried under vacuum (237 mg, 77%). Anal. Calcd for [Mn(NITImH)(NITIm)]ClO_4, $C_{20}H_{29}ClN_8O_8$: C, 40.04; H, 4.87; N, 18.68; Mn, 9.16. Found: C, 40.29; H, 4.92; N, 18.78; Mn, 8.98.

Magnetic Measurements. Magnetic susceptibility data were collected by use of a Quantum Design SQUID susceptometer working at a 0.5 T field strength in the 2−400 K temperature range. The SQUID outputs were corrected for the contribution of the sample holder, and the magnetic susceptibilities were corrected for the diamagnetic contribution of the constituent atoms by use of Pascal's constants.

Low-temperature and high-field measurements were performed at the CRTBT (CNRS, Grenoble, France) by use of homemade apparatus.

X-ray Data Collection and Structure Determination. Crystals of approximate dimensions $0.2 \times 0.1 \times 0.1$ mm^3 were mounted on an Enraf-Nonius CAD-4 four-circle diffractometer equipped with graphite-monochromatized Mo Kα radiation. The unit cell parameters were obtained by least-squares fits of the automatically centered settings from 25 reflections; they are reported in Table 1 with pertinent details regarding the structure determination. Intensity data were corrected for Lorentz and polarization effects but not for absorption.

Structure determinations were performed using methods included in the SHELXTL package of structure determination.[14] The non-hydrogen atoms were located in subsequent Fourier difference maps and refined anisotropically. In the last refinement model, hydrogen atoms were included in fixed and calculated positions with isotropic thermal parameters proportional to those of the connected carbon atoms. In the case of **3**, the uncoordinated nitrato fragment was found disordered.

Atomic positional parameters are listed in Tables 2−5, and selected bond lengths and angles are found in Table 6. Listings of crystal data and experimental parameters, complete bond lengths and angles, anisotropic thermal parameters, and calculated hydrogen coordinates are deposited as Supporting Information.

Results and Discussion

Synthesis. The use of chelating ligands to enforce the coordination of the weakly basic nitroxyl group to weakly acidic metal centers has already been reported and shown to be effective.[11,12] Thus, we were able to characterize discrete four-spin systems involving three imidazolyl-substituted nitronyl nitroxide ligands where the metal coordination sphere is free of ancillary electron-withdrawing groups and is occupied only by organic spin carriers.

Much of the interest in this ligand stemmed from the possibility of ionization of the imidazole group, generating a second symmetrical chelating site. Using such a bis-chelating bridging ligand, the design of extended structures was expected and indeed obtained. In the recently described layered two-dimensional manganese(II) complexes, the metal coordination sphere is fully occupied by only nitroxide ligands.[13] However, the dimensionality of the complexes depends on the base used for

(13) Fegy, K.; Luneau, D.; Paulsen, C.; Ohm, T.; Rey, P. *Angew. Chem.* **1998**, *37*, 1270.

(14) *SHELXTL*, Version 5.030; Siemens Analytical X-ray Instruments: Madison, WI, 1994.

Table 1. Crystallographic Data

	1	**2**	**3**	**4**
chem formula	$C_{12}H_{21}N_4O_6Mn$	$C_{38}H_{46}BN_4O_4S_2Mn$	$C_{13}H_{22}N_7O_7Mn$	$C_{20}H_{29}ClN_8O_8Mn$
fw	372.27	752.68	443.32	599.88
cryst system	orthorhombic	orthorhombic	monoclinic	monoclinic
space group	*Fdd*2	$Pca2_1$	$P2_1/c$	$P2_1/c$
T (K)	293	293	293	293
λ (Å)	0.710 73	0.710 73	0.710 73	0.710 73
ρ_{calcd} (g cm^{-3})	1.515	1.283	1.524	1.440
ρ_{obsd} (g cm^{-3})	1.49(3)	1.32(3)	1.54(3)	1.41(3)
μ (cm^{-1})	8.44	4.88	7.35	6.31
a (Å)	16.713(1)	30.328(3)	9.787(2)	9.761(2)
b (Å)	40.111(3)	13.422(1)	22.973(5)	28.668(5)
c (Å)	9.735(1)	9.589(1)	9.671(2)	9.941(2)
β (deg)	90	90	117.32	96.07(3)
V (Å^3)	6526.3(8)	3903.2(6)	1931.9(7)	2766.2(9)
Z	16	4	4	4
$R(F_o)^a$	0.060	0.085	0.069	0.0371
$R_w(F^2)^b$	0.127	0.145	0.180	0.0655

[a] $R(F_o) = \sum[|F_o| - |F_c|]/\sum|F_o|$. [b] $R_w(F^2) = \{\sum[w(F_o^2 - F_c^2)]/\sum[w(F_o)^2]\}^{1/2}$.

Table 2. Atomic Coordinates ($\times 10^4$) for $[Mn(NITIm)(H_2O)_2]CH_3COO$, **1**

	x	y	z	U(eq)[a]
Mn	0.18035(7)	0.07281(3)	0.66311(14)	0.0262(3)
O1	0.0606(3)	0.05413(13)	0.6183(7)	0.041(2)
O2	−0.1094(3)	0.14485(13)	0.5897(6)	0.034(2)
N1	−0.0025(4)	0.0727(2)	0.6226(8)	0.031(2)
N2	−0.0826(4)	0.1154(2)	0.6092(7)	0.031(2)
N3	0.1343(4)	0.1147(2)	0.5385(8)	0.030(2)
N4	0.0450(4)	0.1531(2)	0.4613(7)	0.029(2)
C1	−0.0082(5)	0.1045(2)	0.5793(8)	0.023(2)
C2	−0.0796(5)	0.0586(2)	0.6771(11)	0.038(2)
C3	−0.1335(5)	0.0899(2)	0.6791(11)	0.032(2)
C4	−0.0654(9)	0.0424(4)	0.813(2)	0.141(8)
C5	−0.1037(7)	0.0328(3)	0.570(2)	0.136(9)
C6	−0.1498(9)	0.1031(2)	0.8185(13)	0.088(5)
C7	−0.2099(7)	0.0861(3)	0.599(2)	0.117(7)
C8	0.0571(5)	0.1235(2)	0.5249(9)	0.026(2)
C9	0.1737(5)	0.1403(2)	0.4826(10)	0.033(2)
C10	0.1204(5)	0.1639(2)	0.4329(11)	0.032(2)
OW1	0.2327(3)	0.04058(13)	0.5124(6)	0.036(2)
OW2	0.1975(4)	0.03284(13)	0.8110(7)	0.044(2)
O3	0.1840(4)	0.0107(2)	0.2804(8)	0.067(2)
O4	0.1557(4)	0.0054(2)	0.0628(8)	0.060(2)
C11	0.1449(5)	0.0177(2)	0.1804(12)	0.039(2)
C12	0.0791(6)	0.0438(3)	0.1937(14)	0.086(5)

[a] U(eq) (Å^2) is defined as one-third of the trace of the orthogonalized $\mathbf{U}_{ij}$ tensor.

deprotonation, on the proportion of reactants, and on the counteranion.

Notably, strong bases such as NaOH only afforded complex mixtures from which we were not able to characterize any compound; it is indeed known that, in the presence of OH^-, manganese(II) is subject to oxidation. In the present case, even in the absence of oxygen, oxidation may occur through metal to ligand electron transfer, which is highly probable in a basic medium. In contrast, compounds **1**−**4** were obtained when weak bases such as manganese(II) acetate or imidazole were used.

The most attractive deprotonation agent is obviously manganese(II) acetate, which acts as both a base and a metal source. Moreover, it was expected that the addition of different sodium salts to the reaction medium would afford extended complexes involving different counteranions and a series of compounds for comparing the magnetic properties. Surprisingly, the 1D complex **1**, where the metal coordination sphere is completed by water molecules and where a noncoordinated acetato group forms a complicated hydrogen-bond network, is generally obtained (Cl^-, NO_3^-, SO_4^{2-}, triflate). Among the counteranions investigated, the only exceptions to this rule were found for ClO_4^-, BPh_4^-, and PF_6^-, for which a layered species was characterized.[13] Worthy of note is the role of the solvent when it is coordinating. Thus, using dimethyl sulfoxide, a 1D complex, **2**, incorporating two solvent molecules in the coordination sphere was characterized. We did not fully investigate the numerous equilibria involved in these reactions, but these observations suggest that they are driven toward the less soluble species depending on the nature of the counteranion and of the solvent.

Use of imidazole as a base led to a different behavior. As expected, excess of base afforded a complex (**3**) where an imidazole group is coordinated but use of the stoichiometric amount of base led to complex **4**, where an additional nonbridging nitroxide completes the coordination sphere. However, using manganese perchlorate, the layered bidimensional complex is obtained in concentrated solutions.

Therefore, the coordination chemistry of this ligand is very rich, allowing us to prepare 1D species involving alternating metal ions and organic free radicals and differing in the nature of the other ligands and of the counteranions.

Structural Studies. In all complexes, the asymmetric unit comprises one metal ion, one deprotonated nitroxide ligand, one counteranion, and two additional coordinated monodentate ligands (in **1**−**3**) or one bidentate ligand (in **4**). As stated previously, these units develop as 1D species where deprotonated ligands bridge manganese(II) ions. These zigzag chains are very similar as illustrated by the distance between nearest metal ions (Mn−MnA) which varies in the range 6.396(2)−6.335(1) Å for **1** and **4**. As shown in Table 7, the presence of different ligands is reflected in slightly different distances between next-neighbor metal ions (Mn−MnB) and more significant differences in the Mn−MnA−MnB angle and in the twist angle (α) between the two rings (imidazolato and imidazoline) of the nitroxide bridging ligand. As expected, in **4** the more sterically demanding pendant nitroxide ligand is responsible for larger Mn−MnA−MnB and α angles. These close similarities are related to stereochemical considerations: the presence of two bis-chelating nitroxides coordinated to each metal ion may indeed result in two stereochemical modifications. One observes the *OC*-6-23, *OC*-6-23, *OC*-6-34, and *OC*-6-21 modifications for **1**−**4**, respectively. Note that these labels correspond to a situation where the two monodentate ligands are arranged in cis positions in **1**−**3** and to the so-called *mer*

Table 3. Atomic Coordinates ($\times 10^4$) for $[Mn(NITIm)(DMSO)_2]BPh_4$, **2**

	x	*y*	*z*	*U*(eq)[a]
Mn	0.68134(7)	0.29315(12)	0.8194(3)	0.0474(6)
O1	0.6563(3)	0.2323(7)	1.0162(11)	0.064(3)
O2	0.7746(4)	0.1594(5)	1.2989(11)	0.048(3)
N1	0.6807(5)	0.1940(7)	1.1138(11)	0.049(4)
N2	0.7353(5)	0.1616(7)	1.2583(13)	0.048(4)
N3	0.7334(4)	0.3449(9)	0.9626(14)	0.050(4)
N4	0.7831(5)	0.3395(9)	1.1269(13)	0.053(4)
C1	0.7227(5)	0.2221(11)	1.149(2)	0.041(4)
C2	0.6600(7)	0.1274(12)	1.225(2)	0.067(5)
C3	0.6310(6)	0.1975(13)	1.313(2)	0.115(6)
C4	0.6323(7)	0.0543(13)	1.148(2)	0.134(10)
C5	0.7015(5)	0.0861(8)	1.2954(14)	0.037(4)
C6	0.6969(5)	0.0869(10)	1.4504(14)	0.061(5)
C7	0.7180(5)	−0.0130(8)	1.245(2)	0.100(8)
C8	0.7462(7)	0.3015(9)	1.082(2)	0.037(4)
C9	0.7658(7)	0.4135(11)	0.941(2)	0.067(6)
C10	0.7961(6)	0.4095(12)	1.040(2)	0.068(5)
S1	0.5859(2)	0.1817(4)	0.7021(7)	0.103(2)
S2	0.6389(2)	0.5134(4)	0.9185(7)	0.132(2)
O3	0.6321(4)	0.2196(7)	0.6987(12)	0.082(4)
O4	0.6412(3)	0.4196(6)	0.8377(11)	0.075(3)
C11	0.5595(6)	0.2437(13)	0.829(3)	0.130(8)
C12	0.5902(7)	0.0630(13)	0.767(2)	0.132(9)
C21	0.5857(7)	0.5564(13)	0.914(2)	0.151(10)
C22	0.6433(8)	0.4837(14)	1.088(2)	0.143(10)
B	0.5940(6)	0.7333(12)	0.367(2)	0.037(5)
C101	0.5565(6)	0.8025(12)	0.448(2)	0.052(5)
C102	0.5501(5)	0.9015(11)	0.417(2)	0.057(5)
C103	0.5207(6)	0.9627(12)	0.490(2)	0.077(6)
C104	0.4964(7)	0.923(2)	0.595(2)	0.088(6)
C105	0.5043(7)	0.825(2)	0.631(2)	0.090(6)
C106	0.5328(6)	0.7655(11)	0.557(2)	0.052(5)
C111	0.5762(6)	0.6143(10)	0.386(2)	0.060(5)
C112	0.5482(6)	0.5739(10)	0.288(2)	0.063(5)
C113	0.5318(6)	0.4742(12)	0.310(3)	0.111(7)
C114	0.5459(8)	0.4135(13)	0.405(3)	0.117(10)
C115	0.5748(7)	0.4537(14)	0.500(2)	0.100(8)
C116	0.5890(6)	0.5468(12)	0.484(2)	0.091(7)
C121	0.6402(5)	0.7457(11)	0.457(2)	0.041(4)
C122	0.6755(6)	0.6793(10)	0.434(2)	0.070(5)
C123	0.7163(7)	0.6918(13)	0.502(3)	0.111(8)
C124	0.7218(7)	0.7659(14)	0.592(2)	0.095(7)
C125	0.6889(7)	0.8298(13)	0.621(2)	0.075(5)
C126	0.6492(6)	0.8189(11)	0.549(2)	0.059(5)
C131	0.5994(7)	0.7655(9)	0.209(2)	0.049(5)
C132	0.6386(7)	0.7666(11)	0.136(2)	0.068(6)
C133	0.6416(9)	0.7914(14)	−0.008(2)	0.104(8)
C134	0.6044(9)	0.8158(12)	−0.082(3)	0.111(9)
C135	0.5651(8)	0.8174(12)	−0.009(2)	0.093(7)
C136	0.5624(8)	0.7924(12)	0.131(2)	0.071(6)

[a] *U*(eq) (Å^2) is defined as one-third of the trace of the orthogonalized $\mathbf{U}_{ij}$ tensor.

modification in **4**, where the metal environment is of the MX_3Y_3 type. In addition, for all complexes, the coordination pattern may result in two enantiomers, but in all cases, one observes a regular alternation of Δ and Λ modifications of the metal coordination spheres along the chain.

However, differences relevant to the understanding of the magnetic properties are found in the crystal packing and intermolecular interactions. Owing to the different space groups, these complexes may be divided into two classes. In **1** the chains are parallel to the diagonals of the *a*,*c* plane while in **2**−**4** they run along the *c* axis. Insight into the structure of these complexes will be obtained on considering in more detail the structures of **1** and **4**.

The asymmetric unit and a fragment of the chain structure of the cationic part of **1** (**1**$^+$) are shown in Figure 2. This unit forms infinite arrays of Mn(II) ions bridged by tetradentate

Table 4. Atomic Coordinates ($\times 10^4$) for $[Mn(NITIm)(H_2O)(ImH)]CH_3COO$, **3**

	x	*y*	*z*	*U*(eq)[a]
Mn	0.1124(2)	−0.15907(7)	0.0461(2)	0.0344(6)
O1	0.0297(10)	−0.1265(3)	−0.1979(9)	0.050(2)
O2	−0.1017(9)	−0.2851(3)	−0.5253(9)	0.040(2)
N1	−0.0354(10)	−0.1597(4)	−0.3201(10)	0.038(2)
N2	−0.0940(11)	−0.2334(4)	−0.4719(11)	0.031(2)
N3	0.1824(10)	−0.2314(4)	−0.0564(10)	0.034(2)
N4	0.1738(11)	−0.2978(3)	−0.2325(10)	0.033(2)
C1	0.0025(12)	−0.2150(5)	−0.3293(13)	0.030(3)
C2	−0.162(2)	−0.1361(6)	−0.465(2)	0.075(5)
C3	−0.2147(14)	−0.1907(5)	−0.5703(12)	0.034(3)
C4	−0.084(4)	−0.0876(10)	−0.513(2)	0.30(3)
C5	−0.278(3)	−0.1084(13)	−0.430(3)	0.27(2)
C6	−0.364(2)	−0.2148(6)	−0.594(2)	0.103(7)
C7	−0.215(2)	−0.1850(7)	−0.725(2)	0.097(6)
C8	0.1180(14)	−0.2470(5)	−0.2083(14)	0.028(3)
C9	0.2775(14)	−0.2749(5)	0.0192(14)	0.042(3)
C10	0.2741(13)	−0.3152(5)	−0.0877(13)	0.039(3)
N5	−0.0173(13)	−0.0864(4)	0.0779(11)	0.040(3)
N6	−0.210(2)	−0.0340(5)	0.062(2)	0.081(4)
C11	−0.170(2)	−0.0849(6)	0.0177(14)	0.048(3)
C12	−0.081(2)	−0.0047(6)	0.150(2)	0.063(5)
C13	0.031(2)	−0.0375(5)	0.159(2)	0.055(4)
OX1	0.4366(13)	−0.0195(5)	0.3278(12)	0.089(4)
NX	0.5167(11)	0.0168(5)	0.283(2)	0.240(14)
OX2	0.578(2)	0.0657(9)	0.365(3)	0.46(3)
OX3	0.536(3)	0.0043(9)	0.158(3)	0.78(6)
OW1	0.3259(9)	−0.1111(3)	0.1183(10)	0.055(2)
OW2	0.419(2)	−0.1169(11)	−0.127(2)	0.216(10)

[a] *U*(eq) (Å^2) is defined as one-third of the trace of the orthogonalized $\mathbf{U}_{ij}$ tensor.

nitroxide ligands where two molecules of water complete the coordination sphere of each metal center. A noncoordinated acetate group ensures charge balance of the complex. All the Mn−O and Mn−N distances are similar, ranging from 2.143(5) Å (Mn−OW1) to 2.254(6) Å (Mn−O2) and from 2.209(7) Å (Mn−N3) to 2.197(6) Å (Mn−N4). The coordination sphere may be described as octahedral, but deviations from this ideal bonding pattern are observed as shown by angles far from those expected for an octahedron (OW1−Mn−N3 = 103.0(3)°, OW2−Mn−N3 = 165.9(2)°). These distortions mainly involve a water molecule, suggesting that this ligand of small size binds in such a way as to minimize steric crowding. As stated previously, the two monodentate ligands are arranged in a cis configuration and a chain is formed of regularly alternating Λ and Δ metal coordination spheres.

These chains are parallel to the [101] or the [$\bar{1}$01] direction. In the *a*,*c* plane, all the chains are parallel so that the crystal may be viewed as alternating planes of parallel chains but the chains in one plane are orthogonal to those of the neighbor planes. The acetate anions are located between the planes and form a complicated net of hydrogen bonds involving the coordinated water ligands; it can be seen that each anion connects three chains belonging to two different planes ($^1/_2 - x$, $-y$, $-^1/_2 + z$) with close contacts (O3−OW1 = 2.683(9), O4−OWB = 2.779(9) Å).

A fragment of the chain structure of **4** is shown in Figure 3. As in **1**, infinite arrays of Mn(II) ions bridged by tetradentate nitroxide ligands are observed, but they all are parallel to the *c* axis and the two monodentate water molecules are replaced by an un-ionized bidentate nitroxide ligand. The metal coordination sphere is also distorted octahedral. The perchlorate counteranions are located between the chains which are thus fairly well separated. Within the distorted octahedral coordination sphere of the metal ion, the Mn−O and Mn−N distances range from

Table 5. Atomic Coordinates ($\times 10^4$) for [Mn(NITIm)(NITImH)]ClO_4, **4**

	x	*y*	*z*	*U*(eq)[a]
Mn	0.06745(8)	0.18152(3)	0.22220(8)	0.0390(3)
O1	0.1423(4)	0.15346(11)	0.4250(4)	0.0521(11)
O2	0.2605(3)	0.27963(12)	0.7037(4)	0.0451(10)
O3	−0.1215(3)	0.14473(12)	0.2233(4)	0.0487(11)
O4	−0.0355(4)	−0.01276(13)	0.2675(4)	0.0697(13)
N1	0.2003(4)	0.1786(2)	0.5223(4)	0.0399(11)
N2	0.2544(4)	0.2379(2)	0.6536(4)	0.0367(12)
N3	0.0056(4)	0.23840(14)	0.3484(4)	0.0396(12)
N4	0.0107(4)	0.28879(14)	0.5245(4)	0.0393(12)
N5	−0.1311(4)	0.1016(2)	0.2591(4)	0.0401(12)
N6	−0.0927(5)	0.0270(2)	0.2812(5)	0.0440(12)
N7	0.1426(5)	0.11360(14)	0.1552(4)	0.0350(11)
N8	0.1603(5)	0.0373(2)	0.1406(4)	0.0482(13)
C1	0.1691(5)	0.2230(2)	0.5473(5)	0.0321(13)
C2	0.2996(6)	0.1572(2)	0.6303(6)	0.048(2)
C3	0.3614(5)	0.2017(2)	0.7024(6)	0.042(2)
C4	0.2085(7)	0.1286(2)	0.7198(7)	0.089(2)
C5	0.3940(7)	0.1253(2)	0.5680(7)	0.099(3)
C6	0.4948(6)	0.2174(2)	0.6533(7)	0.083(2)
C7	0.3761(6)	0.1990(2)	0.8547(6)	0.075(2)
C8	0.0630(5)	0.2499(2)	0.4724(6)	0.0320(12)
C9	−0.0874(6)	0.2728(2)	0.3182(6)	0.056(2)
C10	−0.0860(6)	0.3029(2)	0.4237(6)	0.059(2)
C11	−0.0435(5)	0.0675(2)	0.2347(5)	0.0326(14)
C12	−0.2387(6)	0.0871(2)	0.3476(6)	0.050(2)
C13	−0.2274(6)	0.0325(2)	0.3381(6)	0.048(2)
C14	−0.3770(6)	0.1076(2)	0.2889(7)	0.076(2)
C15	−0.1926(7)	0.1070(2)	0.4870(6)	0.085(2)
C16	−0.2205(7)	0.0068(2)	0.4722(6)	0.079(2)
C17	−0.3359(6)	0.0106(2)	0.2355(6)	0.072(2)
C18	0.0827(5)	0.0733(2)	0.1762(5)	0.0329(13)
C19	0.2637(6)	0.1023(2)	0.1054(6)	0.045(2)
C20	0.2756(6)	0.0554(2)	0.0952(6)	0.056(2)
Cl	0.3348(2)	−0.07879(5)	0.1368(2)	0.0526(4)
O5	0.3552(4)	−0.0473(2)	0.2473(5)	0.089(2)
O6	0.4515(5)	−0.0759(2)	0.0662(5)	0.126(2)
O7	0.2132(4)	−0.0659(2)	0.0533(4)	0.089(2)
O8	0.3228(5)	−0.1241(2)	0.1887(5)	0.101(2)

[a] *U*(eq) (Å^2) is defined as one-third of the trace of the orthogonalized $\mathbf{U}_{ij}$ tensor.

Table 6. Selected Bond Lengths (Å) and Angles (deg)

	1	**2**	**3**	**4**
Mn−O1	2.181(5)	2.19(1)	2.244(8)	2.221(4)
Mn−N3	2.209(7)	2.20(1)	2.201(9)	2.182(4)
Mn−O2A	2.254(6)	2.25(1)	2.277(8)	2.213(3)
Mn−N4A	2.197(6)	2.23(1)	2.174(9)	2.160(4)
Mn−OW1	2.143(5)	2.13(1)	2.172(8)	2.126(4)
Mn−OW2	2.174(6)	2.10(1)	2.214(9)	2.208(4)
O1−N1	1.293(8)	1.30(1)	1.30(1)	1.288(5)
O2−N2	1.276(8)	1.26(1)	1.28(1)	1.296(5)
O1−Mn−N3	80.3(2)	80.2(5)	79.5(3)	80.4(2)
O2A−Mn−N4A	80.8(2)	82.1(5)	80.8(3)	82.3(1)
OW1−Mn−OW2	87.4(2)			
O3−Mn−04		90.8(4)		
OW1−Mn−N5			96.6(4)	
O3−Mn−N7				83.1(2)
O1−Mn−N4A	173.8(2)	170.3(5)	171.6(3)	175.4(2)
O1−Mn−OW1	91.8(2)	92.9(5)	90.0(3)	91.0(2)
O1−Mn−OW2	90.0(2)	91.6(4)	86.5(3)	82.3(2)
O2A−Mn−N3	83.1(3)	83.1(4)	82.7(3)	87.8(1)
O2A−Mn−OW1	171.9(2)	178.9(4)	176.0(3)	175.5(1)
O2A−Mn−OW2	87.6(2)	90.0(4)	87.0(4)	96.1(2)
OW1−Mn−N3	103.0(3)	96.2(4)	94.3(3)	94.3(2)
OW1−Mn−N4A	93.2(2)	97.1(5)	97.0(3)	93.5(2)
N3−Mn−N4A	95.0(2)	94.8(6)	95.3(3)	99.7(2)
OW2−Mn−N3	165.9(2)	170.2(5)	162.2(4)	162.5(2)
OW2−Mn−N4A	93.9(2)	91.1(5)	97.3(3)	97.7(2)

2.126(4) Å (Mn−O3) to 2.221(4) Å (Mn−O1) and from 2.208(4) Å (Mn−N7) to 2.160(4) Å (Mn−N4), the shortest Mn−O and the largest Mn−N bond lengths involving the pendant unionized ligand. Conformational differences between the bridging and pendant ligands are well characterized by the intraligand angles between the imadazole and the imidazoline rings, which are 20.4(3) and 10.6(5)° respectively. It is likely that steric constraints are more demanding for the bridging ligand; this situation results in a higher distortion of the molecule.

Table 7. Structural Parameters Involving Nonbonded Atoms

	1	**2**	**3**	**4**
Mn−MnA (Å)	6.396(2)	6.351(3)	6.392(2)	6.335(1)
Mn−MnB (Å)	9.671(2)	9.589(2)	9.671(2)	9.941(2)
Mn−MnA−MnB (deg)	98.2(2)	98.0(2)	98.3(2)	103.1(3)
α[a] (deg)	18.4	11.0	17.3	20.4
				10.6[b]
Mn−O−N (deg)	122.9(2)	124.7(3)	122.0(3)	119.4(2)
MnA−O−N (deg)	122.9(2)	125.0(2)	123.5(3)	123.7(2)
				123.6(3)[b]
β[c] (deg) Mn	34.2	32.5	34.4	40.7
MnA	38.4	35.7	34.8	32.7
				37.3[b]

[a] Angle between the imidazole and the imidazoline rings in the nitroxide ligands. [b] In the pendant ligand. [c] Angle between the M−O−N plane and the imidazoline plane of the ligand.

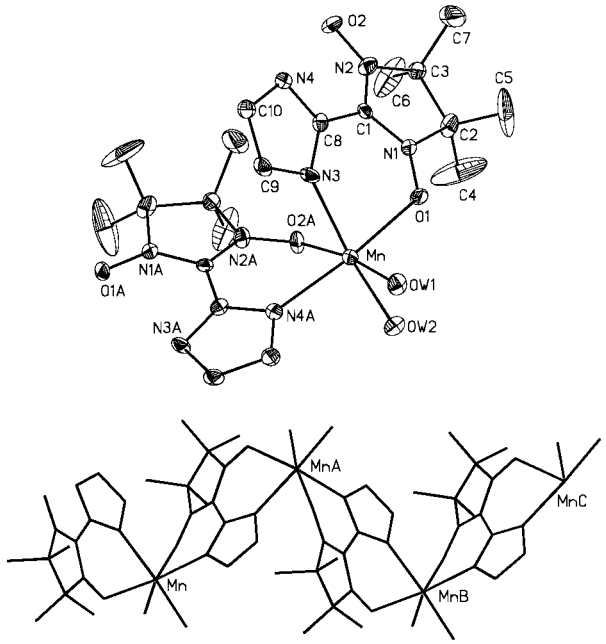

Figure 2. Cationic part of the asymmetric unit and fragment of the chain structure for **1**. Thermal ellipsoids are drawn at the 30% probability level.

In compound **4**, it is seen readily that only the *mer* isomer is present. In contrast, the discrete complex involving three unionized nitroxide ligands exists preferably as the *fac* modification. It has been shown that such a *fac* arrangement observed in the solid state was the result of a delicate balance between steric crowding around the metal ion and crystal packing interactions. Although a *fac* arrangement does not minimize local steric interactions, it maximizes the compactness of the crystal. In the case of **4**, only the first criterion holds so that the *mer* modification is favored. On examining Figure 3, one sees that the corresponding *fac* modification of compound **4** would be obtained on exchanging the positions of the coordinated oxygen and nitrogen atoms of each pendant ligand, a modification which does not alter the chirality of the metal coordination spheres. Computer modeling of such a *fac* isomer shows that, in this geometry, shorter contacts between methyl

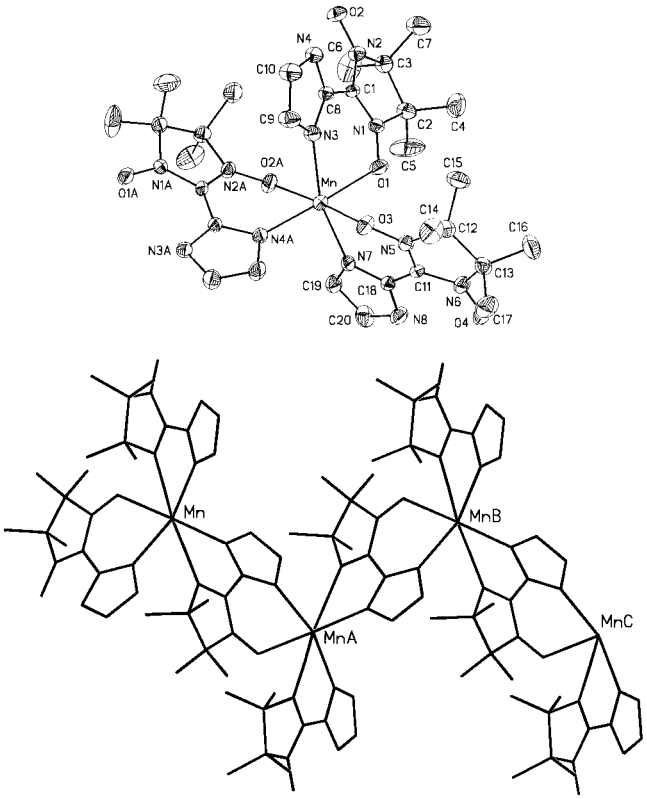

Figure 3. Cationic part of the asymmetric unit and fragment of the chain structure for **4**. Thermal ellipsoids are drawn at the 30% probability level.

groups of pendant and bridging ligands (3.1 Å) would take place; therefore, release of steric constraints is probably the cause of the preferred *mer* arrangement in this chain compound. Examination of Figure 3 also shows that the pendant ligands alternate regularly along the chain, their positioning being tentatively described as trans. The opposite situation with all pendant ligands on the same side of the chain would be obtained with manganese coordination spheres of same chirality and would result in other short intramolecular contacts between adjacent pendant ligands.

These considerations do not apply for the cis compounds **1**−**3** where, obviously, a trans configuration involving achiral centers would be favored, considering only steric crowding. It can be tentatively proposed that a Δ, Λ alternation within a chain is the less energetic way to build a racemic crystal. Therefore, although the discrete compound exists as the *fac* modification, it is likely that a cis or *mer* arrangement and a Δ, Λ alternation minimize steric constraints arising from the chain structure in **1**−**4**. Such a chiral Δ, Λ pattern is common and has been observed in the analogous layered complex $[Mn_2(NITIm)_3]_\infty$[13] and in related planar polymetallic structures which can be viewed as parallel zigzag chains linked to form a hexagonal net.[7,8,15−17] In this net, the interchain links are trans and adjacent manganese octahedrons are of opposite chirality. Concerning chirality, further interesting comparisons with the discrete compound can be made. In the solid state, the discrete molecular units are linked by perchlorate anions through hydrogen bonds involving the imidazole nitrogen in such a way that chains are

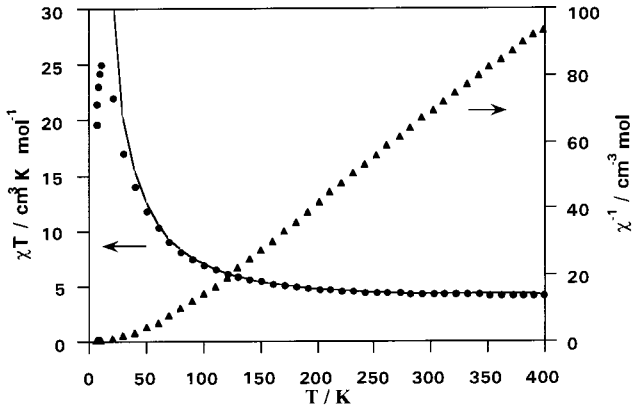

Figure 4. Temperature dependence of χT (●) and $1/\chi$ (▲) for complex **1**.

Table 8. Magnetic Parameters

	1	**2**	**3**	**4**
T_{min} (K)	380(6)	378(6)	380(6)	252(5)
J_1[a] (cm^{-1})	45(4)	43(3)	46(4)	49(4)
J_2 (cm^{-1})				86(5)
T_c (K)	4.8	1.9	4.3	4.5

[a] $H = -2J\mathbf{S}_i\cdot\mathbf{S}_j$.

running along the *b* axis. Within a chain, all the coordination spheres exhibit the same chirality. As a consequence, each chain is surrounded by chains of opposite optical activity, leading to a racemic crystal. Contrastingly, in **1**−**4**, within each chain, Λ and Δ octahedrons alternate, resulting also in the racemate.

Magnetic Studies. The temperature dependence of the product of the magnetic susceptibility with the temperature in the 2−400 K temperature range is displayed in Figure 4 for compound **1**. When the temperature is lowered, χT decreases to a minimum at 380(6) K (4.22 cm^3 K mol^{-1}, 5.81 μ_B), then increases, reaching a maximum at 10 K ($\chi T = 25$ cm^3 K mol^{-1}, $\mu = 14.1$ μ_B), and finally decreases. Upon a return to higher temperatures, the same behavior is observed. Qualitatively, the presence of the minimum at 380 K is the signature of antiferromagnetic interactions between organic and metal spins leading to a ferrimagnetic chain; the overall behavior is similar to that of several manganese−copper[18,19] or manganese−nitroxide[20,21] chain compounds already reported. The presence of manganese−nitroxide antiferromagnetic interactions is also confirmed by the value of χT at 400 K ($\chi T = 4.26$ cm^3 K mol^{-1}, $\mu = 5.8$ μ_B), which is lower than that corresponding to uncorrelated spins (4.75 cm^3 K mol^{-1}), and by the field dependence of the magnetization at 10 K, which reaches saturation at 22 200 cm^3 G mol^{-1} (3.97 μ_B), in agreement with an $S = 2$ ground spin state for the asymmetric unit. A similar antiferromagnetic behavior was observed for the discrete manganese complex whose χT vs *T* curve exhibits a plateau at low temperature, consistent with an $S = 1$ ground spin state. These features are almost identical to those observed for compounds **2** and **3**, whose χT vs *T* curves exhibit the minima of χT reported in Table 8.

For compound **4**, a similar behavior is also observed (Figure 5), except that the minimum of χT appears at a lower

(15) Mathonière, C.; Nuttall, C. J.; Carling, S. G.; Day, P. *Inorg. Chem.* **1996**, *35*, 1201.
(16) Stumpf, H. O.; Ouahab, L.; Pei, Y.; Grandjean, D.; Kahn, O. *Science* **1993**, *261*, 447.
(17) Carling, S. G.; Mathonière, C.; Day, P.; Malik, K. M. A.; Coles, S. J.; Hursthouse, M. B. *J. Chem. Soc., Dalton Trans.* **1996**, 1839.
(18) Kahn, O.; Pei, Y.; Verdaguer, M.; Renard, J.-P.; Sletten, J. *J. Am. Chem. Soc.* **1988**, *110*, 782.
(19) Kahn, O.; Pei, Y.; Journaux, Y. In *Inorganic Materials*; Bruce, D. W., O'Hare, D., Eds.; J. Wiley and Sons: New York, 1992; p 59.
(20) Caneschi, A.; Gatteschi, D.; Renard, J.-P.; Rey, P.; Sessoli, R. *Inorg. Chem.* **1989**, *28*, 1976.
(21) Caneschi, A.; Gatteschi, D.; Renard, J.-P.; Rey, P.; Sessoli, R. *Inorg. Chem.* **1989**, *28*, 2314.

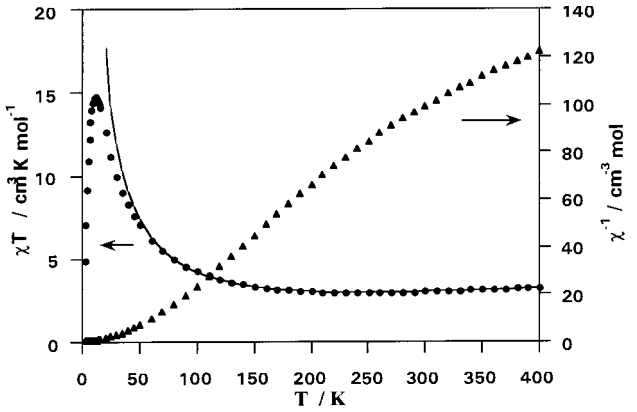

Figure 5. Temperature dependence of χT (●) and $1/\chi$ (▲) for complex **4**.

temperature (252(5) K) and that the magnetization saturates at 16 300 cm^3 G mol^{-1} (2.92 μ_B), in agreement with an $S = {}^3/_2$ ground spin state.

Further information regarding the magnetic behavior of these complexes comes from the temperature dependence of χ and $1/\chi$. It is seen for all compounds that χ does not exhibit any maximum and that its low-temperature values are field dependent. Thus, it is inferred that the maximum observed in the χT vs T curves is probably the consequence of saturation effects. For compounds **1**−**3**, $1/\chi$ exhibits a linear dependence with the temperature which, surprisingly, intercepts the temperature axis at large and positive Θ values of 49, 46, and 48 K, respectively. Indeed, the metal−radical interaction is antiferromagnetic, and one would expect to observe a Curie−Weiss law including a negative value of Θ.[22] This feature is well explained as follows: a regular Curie−Weiss behavior would be observed at higher temperature; well below the minimum of χT (380 K), in the 300−100 K temperature range, where the behavior of $1/\chi$ is linear, one observes short-range order between effective spins which are almost parallel as a consequence of the ferrimagnetic structure.[23]

The study of the magnetic properties will be divided in two parts: (i) the high-temperature behavior with the characterization of the coupling constants involving nitroxide ligands and manganese(II) ions and (ii) the low-temperature magnetic behavior with the characterization of macroscopic properties.

High-Temperature Behavior. Modeling of ferrimagnetic chains, including alternating $S = {}^5/_2$ and $S = {}^1/_2$ spins, has been successfully achieved.[18,23] However, these 1D systems are far more complicated than the regular species described in the literature. In **4**, the presence of the pendant paramagnetic ligand has not been considered previously and, even in compounds **1**−**3**, possible exchange pathways are numerous. Indeed, within a chain one may expect (i) large and antiferromagnetic direct coupling between bound manganese(II) ions and organic radicals,[20,21,24] (ii) a probably weaker competing interaction between manganese ions via a superexchange pathway through the bridging imidazole fragment,[25] and (iii) due to the cis conformation, through-space direct intramolecular interactions within the metal coordination spheres between the nitroxide ligands (O1A−O1B = 3.29(4) Å) which are difficult to estimate.[26,27] Although the discrete compound and the chain compounds differ in being isomeric (*fac* and *mer*, respectively), the understanding of the magnetic properties of the former helps in modeling local magnetic interactions within the asymmetric unit of the latter. This study indeed showed that, considering only a manganese−nitroxide interaction, the quality of the fitting process was almost independent of the value of the nitroxide−nitroxide interaction. Therefore, it was assumed that the high-temperature magnetic behaviors of the 1D complexes **1**−**4** could be described by considering only interactions between linked spin carriers.

Owing to the presence of two inequivalent nitroxide ligands in the asymmetric unit of **4**, we developed a model similar to those reported for alternating ${}^5/_2$ and ${}^1/_2$ antiferromagnetically coupled spins[23,24] but including the additional pendant nitroxide ligand.

The magnetic behavior of **4** can be represented in a schematic way by the Hamiltonian

$$H = \sum_{i=1}^{N} H_i \tag{1}$$

with

$$H_i = -2J_1\mathbf{s}_i\cdot(\mathbf{S}_i + \mathbf{S}_{i+1}) - 2J_2\mathbf{S}_i\cdot\mathbf{s}_i' \tag{2}$$

where $\mathbf{S}_i$ are the Mn(II) $S_i = {}^5/_2$ spins while $\mathbf{s}_i$ and $\mathbf{s}_i'$ are the nitroxide $s_i = s_i' = {}^1/_2$ spins. The $\mathbf{s}_i$ spins are along the chain, while the $\mathbf{s}_i'$ spins are those of the pendant nitroxide.

A quantum resolution of H is a very difficult task, and a semiclassical model was used in which the $\mathbf{S}_i$ are treated as classical spins with modulus S and the nitroxide spins $\mathbf{s}_i$ and $\mathbf{s}_i'$ are considered as quantum spins. We successively evaluated the classical correlations $\langle S_i^Z S_{i+p}^Z\rangle$, the quantum classical correlations $\langle S_i^Z s_{i+p}^Z\rangle$ and $\langle S_i^Z s_{i+p}'^Z\rangle$, and the quantum correlations $\langle s_i^Z s_{i+p}^Z\rangle$, $\langle s_i'^Z s_{i+p}^Z\rangle$, and $\langle s_i'^Z s_{i+p}'^Z\rangle$. The magnetic susceptibility is given according to the linear response theory by:

$$\chi = (g^2\mu_B{}^2/kT)\sum_{i,j}\langle(S_i^Z + s_i^Z + s_i'^Z)(S_j^Z + s_j^Z + s_j'^Z)\rangle \tag{3}$$

Setting

$$x = -(2J_1S/kT), \quad x_2 = -(2J_2S/kT) \tag{4}$$

$$d = (a_1/3a_0), \quad L = (b_1/3a_0) + (b_0/a0), \quad t = \tanh(x_2/2) \tag{5}$$

with

$$a_0 = 4x_1{}^{-2}(x_1\sinh x_1 - \cosh x_1 + 1) \tag{6a}$$

$$a_1 = 12x_1{}^{-4}[(x_1{}^3 + 12x_1)\sinh x_1 - 5(x_1{}^2 + 12)\cosh x_1 - x_1{}^2 + 12] \tag{6b}$$

$$b_0 = x_1{}^{-1}(\cosh x_1 - 1) \tag{6c}$$

$$b_1 = 3x_1{}^{-3}[(x_1{}^2 + 4)\cosh x_1 - 4x_1\sinh x_1 + x_1{}^2 - 4] \tag{6d}$$

we obtain for a chain of N magnetic units

(22) Carlin, R. L. *Magneto-chemistry*; Springer-Verlag: Berlin, 1986.
(23) Seiden, J. *J. Phys. Lett.* **1987**, *44*, 947.
(24) Belorizky, E.; Rey, P. *Mol. Phys.* **1992**, *75*, 563.
(25) Kolks, G.; Lippard, S. J.; Waszczak, J. V.; Lilienthal, H. R. *J. Am. Chem. Soc.* **1982**, *104*, 717.
(26) Lanfranc de Panthou, F.; Luneau, D.; Laugier, J.; Rey, P. *J. Am. Chem. Soc.* **1993**, *115*, 9095.
(27) Pei, Y.; Lang, A.; Bergerat, P.; Kahn, O.; Fettouhi, M.; Ouahab, L. *Inorg. Chem.* **1996**, *35*, 193.

$$\chi = \frac{Ng^2\mu_B{}^2}{3kT}\left[S^2 + s(s+1) + s'(s'+1) - St + \frac{1}{1-d}(-4SL + 2L^2 + 2Lt) + \frac{d}{1-d}\left(2S^2 - 2St + \frac{t^2}{2}\right)\right] \quad (7)$$

Because the value of S has not been specified, expression 7 reduces to that reported by Seiden when $J_2 = 0$ ($t = 0$) and $s' = 0$.[23]

The derivation of (7) is detailed in a forthcoming paper in which it is shown that when S is considered as a classical spin, the resulting correlation functions involving **S** are much closer to their exact quantum values when $S = [S(S+1)]^{1/2}$; i.e., $S = (35/4)^{1/2}$ for Mn(II) rather than $S = {}^5/_2$. Thus, eq 7 was used for the interpretation of the magnetic susceptibility of **4** with $S = (35/4)^{1/2}$ and $s = s' = {}^1/_2$. For compounds **1**−**3**, $s' = 0$ ($J_2 = 0$). This expression is expected to provide a satisfactory description of the magnetic behavior in a temperature range such that x_1 and x_2 do not exceed a value of about 5.

Considering only the high-temperature data (>100 K) and fixing the g value to 2, we obtain the best-fit values displayed in Table 8. Note that the minima of χT are well reproduced by the model. The coupling constants (≈50−80 cm^{-1}) compare well with those observed in the discrete manganese(II) derivative of the same ligand, but they are much weaker than those observed in reported manganese(II)−nitroxide unidimensional or cis-coordinated complexes where the nitronyl nitroxide ligands are bound only by the nitroxyl oxygen atoms. The structural and magnetic consequences of coordination through a chelating mode were discussed previously and afford a qualitative understanding of the weakening of the coupling constant.[12] However, modeling of the magnetic properties of the chain compounds did not take into account the additional coupling pathway of the adjacent manganese ions through the imidazole ring. Indeed, considering two manganese ions, coupling of both ions to the unpaired spin of the bridging radical results in parallel metal spins while indirect coupling through the imidazole ring results in the opposite situation. The latter interaction is expected to be weak so that the behavior of the chain is ferrimagnetic; however, it is likely that the coupling constants thus determined are slightly underestimated.

Low-Temperature Behavior. At low-temperature, complexes **1**−**4** exhibit closely related magnetic properties, which are reported in detail for **4**. In Figure 6 is shown the temperature dependence of the initial magnetic susceptibility as recorded with an ac mutual inductance bridge working at 119 Hz in a 0.1 Oe field. Deviation from Curie law behavior is observed below 10 K, and a tendency to saturation is observed around 5 K. These effects are well understood as being the consequence of antiferromagnetic interactions. However, on decreasing the temperature, one observes a sharp increase of χ' at 4.5 K, which is the signature of ferromagnetic interactions; at lower temperatures (<2.4 K), the ac susceptibility decreases and tends to an extrapolation of the curve observed above 5 K. Concomitantly, the out-of-phase component, χ'', of the susceptibility exhibits two distinct peaks at 4.3 and 3.1 K which may correspond to two different ferromagnetic phases or to two spin−lattice relaxation processes of the same phase.[28,29]

To better understand this behavior, we studied the low-field (0−0.3 T) magnetization of this system in the 50 mK−10 K temperature range. A few curves are displayed in Figure 7. At 4.2 K, the magnetization exhibits a strong initial variation of $M(H)$ which is fully consistent with the high value of χ' at the same temperature. On increasing the field strength, one observes a saturation behavior corresponding to a small fraction of the total expected magnetization. These two features are characteristic of the onset below 4.5 K of a weak ferromagnetic component. Below 4.2 K, a hysteresis loop appears whose coercive field increases rapidly to reach 300 Oe at 0.08 K. Note that the initial value of the susceptibility at 0.08 K is much weaker than that at 4.2 K, an effect which is in line with the drop of χ' below 2.5 K observed in Figure 6. On increasing the magnetic field up to 0.2 T, one sees an upward curvature of the magnetization which is consistent with the already mentioned presence of antiferromagnetic interactions (vide infra) progressively overcome by the magnetic field. As gauged by the value of the magnetization at saturation, the ferromagnetic component is very weak since it corresponds to only 1.5% of the expected saturation magnetization. To ensure that impurities are not at the origin of such a low ferromagnetic component, we studied several samples which all show the same behavior and reproducible measurements.

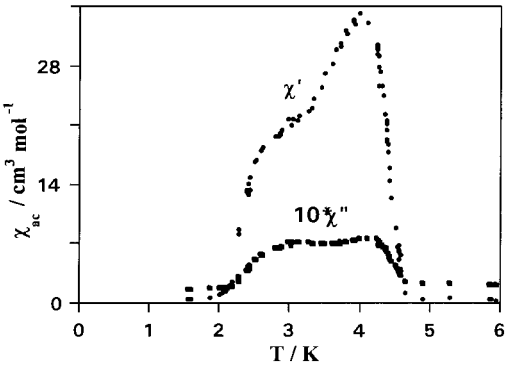

Figure 6. Temperature dependence of the in-phase (χ') and the out-of-phase component (χ'') of the ac susceptibility for compound **4**.

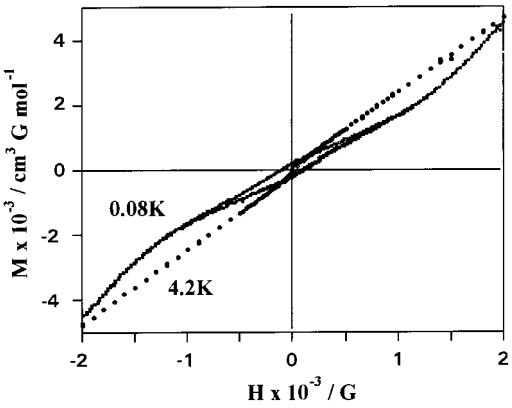

Figure 7. Cycled field dependence of the magnetization at 4.2 (●) and 0.08 K (• • •) for compound **4**.

Important information is also gained from "zero-field-cooled" (ZFC) and "field-cooled" (FC) measurements as illustrated in Figure 8 for an applied field of 5 Oe. The onset of a hysteresis loop is confirmed by a difference between the ZFC and the FC magnetization curves. On examining the data displayed in this figure, one obtains an ordering temperature of 4.3 K, consistent with the high-temperature peak in χ''. In conclusion, at low temperature this complex behaves as a weak ferromagnet.

Such an ordered phase has been observed in structurally related 1D materials[30,31] as a result of in-chain and interchain coupling and local anisotropy. In the present case, at low

(28) Van Duynevelt, A. J. *Magnetic Molecular Materials*; NATO ASI Series, No. 198; Kluwer Academic Publishers: Dordrecht, The Netherlands, 1990; p 353.
(29) Turner, S.; Kahn, O.; Rabardel, L. *J. Am. Chem. Soc.* **1996**, *118*, 6428.

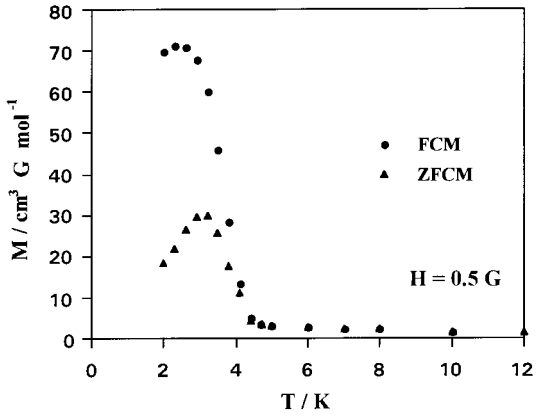

Figure 8. Zero-field-cooled (▲) and field-cooled (●) curves for compound **4**.

temperature the ferrimagnetic chains may be schematized as effective spins carried by manganese ions. Two adjacent manganese sites are related by a plane of symmetry (and a translation) so that they have different chiralities and they also have different magnetic anisotropies. Although the Mn(II) ion is usually highly isotropic, the coordination spheres within a chain are indeed distorted in different ways, leading to magnetically inequivalent adjacent metal ions. These ferrimagnetic chains involving inequivalent metal ions are weakly antiferromagnetically coupled, as shown by the low-temperature measurements, because they are connected by hydrogen bonds. Therefore, at low temperature, where this interaction is operative, the compounds exhibit a nonvanishing weak magnetic moment.

For compounds **1**−**3**, similar behaviors are observed but different ordering temperatures reflecting the different structures of the complexes were determined. In particular, compound **2**, in which the dimethyl sulfoxide ligands and the BPh_4 anion are not expected to efficiently connect the chains, orders below 2 K.

Conclusion

Compounds **1**−**4** are the first examples of 1D molecular magnetic materials involving nitroxide free radicals and transition metal ions where the coordination sphere of the metal centers is free of ancillary electron-withdrawing groups. These complexes are derivatives of a chelating ligand including an imidazole group which can be deprotonated. Although difficult to control, the coordination chemistry of this ligand is rich in giving numerous compounds differing in additional ligands and counteranions. Of particular interest is compound **4**, where only nitroxide ligands are present in the environment of the metal ion. Since in all complexes adjacent metal centers are of opposite chirality, complex **4** is a 1D precursor of a bidimensional species which would be obtained by deprotonation of the un-ionized pendant ligand. We recently reported that this was indeed possible.[13] Seeking a three-dimensional structure which would involve metal centers of the same chirality, we are investigating the coordination chemistry of chiral imidazolyl-substituted nitroxides.

These complexes are weak ferrimagnets exhibiting ordering temperatures lower than 5 K. Since three-dimensional ordering depends on the metal anisotropy, we are currently investigating analogous complexes of Co(II) where strong single-ion anisotropy could lead to larger ordering temperatures.

Acknowledgment. Support from European Community HCM Program CHRX CT920080 and INTAS Program 94-3805 is gratefully acknowledged.

Supporting Information Available: Listings of crystallographic data, bond lengths, bond angles, anisotropic parameters, and calculated hydrogen coordinates for **1**−**4** (24 pages). Ordering information is given on any current masthead page.

IC971619D

(30) Martinez-Lorente, M. A.; Tuchagues, J.-P.; Pétrouléas, V.; Savariault, J.-M.; Poinsot, R.; Drillon, M. *Inorg. Chem.* **1991**, *30*, 3589.
(31) Day, P. *J. Chem. Soc., Dalton Trans.* **1997**, 701.